



## Synthesis, Equilibria, Dft and Biological Investigation of Homopiperazine Complex with Diphenyltin(IV)

Amira M. Abdel Wahab, Mohamed M. Shoukry\*, Mohamed R. Shehata and Perihan A. Khalf-Alla



Department of Chemistry, Faculty of Science, Cairo University, Giza, 12613, Egypt

### Abstract

The diphenyltin(IV) dichloride complex with 1,4-diazacycloheptane (Homopiperazine) was prepared. Elemental micro-analysis, mass spectral, thermal and spectral measurements were used to reveal the complex structure. The 1:1 complex is formed through coordination of the nitrogen atoms of homopiperazine to Sn. The equilibria involved in the complex formation in solution were investigated. The complexes detected in solutions are of stoichiometric ratio 1:1, including the protonated and hydrolyzed species. The complexes formation constants were estimated using the potentiometric data and the non-linear computer program Miniquad-75. Density Functional Theory (DFT) calculations have been executed to study the equilibrium geometry of homopiperazine and its diphenyltin(IV) complex. The optimization of the diphenyltin(IV) complex structure reveals that the Sn atom is six-coordinate in an octahedral geometry with some distortion where the homopiperazine nitrogen atoms and the two chloride ions are in one plane. The distance between the two nitrogen atoms in the uncomplexed homopiperazine is 3.149 Å and decreased to 2.585 Å in the complex. Bonds connected to N atoms are lengthened upon complex formation. Homopiperazine and its complex were screened against antimicrobial *Staphylococcus aureus* (+ve), *Escherichia coli* (-ve) and against antifungal *Candida albicans* and *Aspergillus flavus*. Antitumor activities of homopiperazine and its diphenyltin(IV) complexes were tested against breast cancer cell lines. Docking studies confirm the experimental results

Keywords: diphenyltin(IV) complexes, homopiperazine, Equilibrium constants, DFT, Docking, Biological studies

### 1. Introduction

Organotin(IV) complexes have received significant attention in the last two decades due to their pronounced activity in agriculture and medicine. These complexes have potential biological activities as antitumor [1-5], anti-inflammatory [6], antibacterial [7], antifungal [8], and anti-insecticidal effects [9].

*Cis-platin*, the first platinum-based antitumor drug, has clinical achievements. Many researchers have extensively investigated non-platinum-based chemotherapeutics to improve therapeutic activity and aiming to prevent severe side effects of platinum-based drugs. Organotin(IV) complexes are considered as interesting metallodrugs, as they show better

biological effect than *cis-platin* [4,10-14]. Also, they have higher antitumor effect with lower toxicity, good excretion properties. The Organotin(IV) complexes exhibit less side effects than those of many platinum-based drugs, even when used in lower concentrations [15-17]. Also, they have good selectivity toward various cancer cell lines [18,19].

In continuance with our previous investigations on organotin(IV) compounds [20-29], the present study is directed to investigate the diphenyltin dichloride complex with a bidentate amine having structural feature enhancing the biological activity. The amine investigated is homopiperazine, it has hydrophobic nature which may help its diphenyltin(IV) complex to pass into the biological cell and consequently

1 Bloom, J., Mamluk Art and Architectural History: A Review Article, Middle East Documentation Center, The University of Chicago, 2012, p. 31.

\*Corresponding author e-mail: [shoukrymm@hotmail.com](mailto:shoukrymm@hotmail.com); (Mohamed M. Shoukry).

Receive Date: 04 December 2021, Revise Date: 10 December 2021, Accept Date: 12 December 2021

DOI: 10.21608/EJCHEM.2021.109334.4987

©2022 National Information and Documentation Center (NIDOC)

developed biological activity. Also, the phenyl groups bound to Sn(IV) may undergo stacking interaction with biological ligands. In the present study, the speciation of the complexes will be investigated. The obtained equilibrium data will support the biological importance of the complex. The solid complex will be prepared, and the structure is evidenced by spectral and thermal measurements. Density Functional Theory (DFT) investigation was achieved to catch the geometries of homopiperazine and its complex. The biological activity of the homopiperazine and its diphenyltin(IV) complex was tested and results were compared with those obtained by docking analysis

## 2. Experimental

### 2.1 Materials and reagents

Diphenyltin(IV) dichloride (DPT) was purchased from Alfa Aesar Chem. Co. Homopiperazine ligand (HP) was provided from Sigma Chem. Co. 1,4-Dioxane was from by Aldrich Chem. Co. BDH concentrated volumetric solutions vials was used to prepare sodium hydroxide solutions by dilution. The concentration of sodium hydroxide solutions were regularly checked by titration against potassium hydrogen phthalate.

The diphenyltin(IV) dichloride-homopiperazine complex was synthesized by mixing homopiperazine (1mM, 0.10 gm) and (Ph)<sub>2</sub>SnCl<sub>2</sub> (1mM, 0.34 gm) in 20 ml methanol. The mixture was stirred for 2 hours. The formed precipitate was separated by filtration and washed thoroughly with diethyl ether. (Yield 89%). Anal. Calcd for C<sub>17</sub>H<sub>22</sub>SnN<sub>2</sub>Cl<sub>2</sub> (M.Wt 443.99): Calcd. C, 45.99; H, 4.99; N, 6.31. Found, C, 45.0; H, 5.2; N, 6.2.

### 2.2. Procedure and Measuring Techniques

The solid complex composition was evidenced by elemental analysis; Analysis of carbon, hydrogen and nitrogen was carried out on a Perkin-Elmer 240C elemental analyzer. Infrared spectra were obtained by 8001-PC FT-IR Shimadzu spectrophotometer using KBr pellets in the mid-infrared region 4000-400 cm<sup>-1</sup>. The mass spectrum was recorded by EI ionization mode using MS-5988 GS-MS Hewlett-Packard instrument at 70 eV. Thermal analysis (TGA and DTA) were performed in a nitrogen atmosphere with TGA-50 Shimadzu thermogravimetric analyzer and DTA-50 Shimadzu differential thermal analyzer. The potential characteristics are as follows: Heating rate: 10K min<sup>-1</sup>, Sample size: 10-15mg for TAG and 20mg

for DTA, A. Temperature range: room temperature to 800° C.

The potentiometric titrations were accomplished by a Metrohm 686 titroprocessor having a 665 dosimat (Switzerland-Herisau). A Metrohm glass-calomel combined electrode, a thermometric probe was used. The titration system was standardized by NBS buffer solutions [30]. The temperature of the titrated solutions was controlled at 25.0±0.1°C by circulation of thermostated water through the jacket of a titration vessel. Sodium nitrate was used to adjust the ionic strength to 0.1 mol dm<sup>-3</sup>. All potentiometric titrations were carried out under a nitrogen atmosphere. homopiperazine solution was prepared in the protonated form by dissolving in HNO<sub>3</sub> solution. The acid-base equilibria of homopiperazine in the protonated form were estimated by titrating 1.25 mmol. The diphenyltin(IV) hydrolysis constants of were estimated by titrating 1.25 mmol. Formation constants of diphenyltin(IV)-homopiperazine complexes were estimated by titrating solution mixture of diphenyltin(IV) (1.25 mmol) and homopiperazine (1.25 mmol). The volume of each titrated solution mixtures was 40 mL. NaOH solution (0.05 mol.dm<sup>-3</sup>) was used as the titrant. The solvent composition was 75% dioxane. The pK<sub>w</sub> values in dioxane-H<sub>2</sub>O solutions were estimated as reported previously [31,32]. For this purpose, various amounts of standard NaOH solution were added to a 0.10M NaCl solution. [OH<sup>-</sup>] was calculated from the amount of base added; [H<sup>+</sup>] was obtained from the pH value. The equilibrium constant of the binary complex was evaluated from titration data. The equilibrium was defined by Eq. 1.



Where M, HP and H represent diphenyltin(IV), homopiperazine and proton respectively.

The formation constants were evaluated using MINQUAD-75 computer program[33]. The composition and stability constants of the complexes possibly formed were estimated by trying various models with different compositions. The accepted model is characterized by having the best statistical fit and should be chemically consistent with the magnitude of various residuals, as reported elsewhere [33]. Table 1 list the equilibrium constants associated with their standard deviation as obtained from the MINQUAD calculation result. The Concentration distribution diagrams were derived by means of the program SPECIES [34].

### 2.3. Molecular modeling studies.

Density Functional Theory (DFT) calculations have been executed to study the equilibrium geometry of the ligand and DPT-HP complex at the B3LYP level of theory, where C, H, N and Cl atoms with basis set 6-311G++(dp) and Sn atom with basis set LANL2DZ, respectively using Gaussian 09 program [35].

### 2.4 Molecular docking

The molecular docking investigations were done using MOA2019 software [36]. The binding modes of the most active site of the receptor of breast cancer oxidoreductase (PDB ID: 3HB5) [37] and of the receptor of *Staphylococcus aureus* (gram -ve bacteria) (PDB ID: 1jjj) [38] were estimated. The optimized structure of HP and diphenyltin(IV) complex from the output of Gaussian09 calculations were created in PDB file format. The crystal structures of the receptors were downloaded from the protein data bank (<http://www.rcsb.org/pdb>).

## 3. Results and discussion

### 3.1. Characterization of the complex

The synthesized diphenyltin(IV) complex was investigated by elemental analysis. The analytical result revealed that the complex is of composition 1:1. The mass spectrum of the complex was studied. It is clear from the spectrum, Fig. 1, that the molecular ion peak agrees with the suggested formula of the complex. This is supporting the elemental analysis.

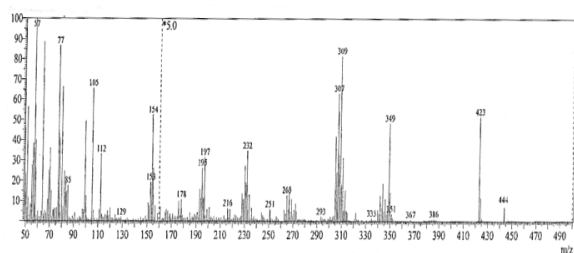


Fig. 1. Mass spectrum of diphenyltin(IV) complex with homopiperazine.

The infrared spectra of free homopiperazine and its complex are given in Figure 2. The characteristic IR spectral bands are compared. The stretching vibration at 3294 cm<sup>-1</sup>(νNH) in the IR spectrum of the free homopiperazine is shifted in the spectrum of the complex to 3423 cm<sup>-1</sup>. The shoulder at 3052 cm<sup>-1</sup> and the broad bands at 2994 and 2940 cm<sup>-1</sup> are due

to νCH stretching of phenyl rings. The broad bands at 3039, 2935 and 2883 cm<sup>-1</sup> corresponding to aliphatic νCH in the free homopiperazine are shifted to 2815, 2752 and 2690 cm<sup>-1</sup> in the complex spectrum. The bending vibrations of (δNH) at 1668 cm<sup>-1</sup> in free homopiperazine are shifted to 1585 cm<sup>-1</sup> in the complex spectrum. The absorption at 567 cm<sup>-1</sup> is for νSn-C in the complex spectrum. The band at 432 cm<sup>-1</sup> in the complex spectrum corresponds to the νSn-N stretching vibration [39]. Therefore, in the complex, homopiperazine is attached to Sn center by the two nitrogen atoms forming a chelate ring.

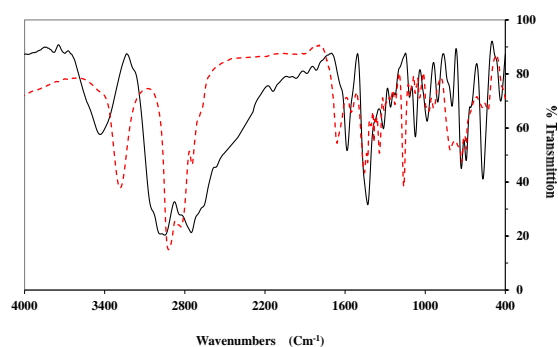


Fig. 2. Infrared spectrum of homopiperazine (---) and Complex (—).

The <sup>1</sup>H NMR spectra of homopiperazine and its diphenyltin(IV) complex were recorded in DMSO-d<sub>6</sub>. The characteristic <sup>1</sup>H NMR signals (δ, ppm) for free homopiperazine protons and complex are shown in Figures 3, Scheme 1 and Table 1. The homopiperazine NH protons signals are shifted downfield by 0.29 ppm due to coordination with Sn(IV). The H(α), H(β) and H(γ) signals were affected by complex formation. They are shifted downfield by values 0.29, 0.42 and 0.32 ppm respectively. These data revealed that homopiperazine nitrogen atoms are coordinated to Sn(IV) atom.

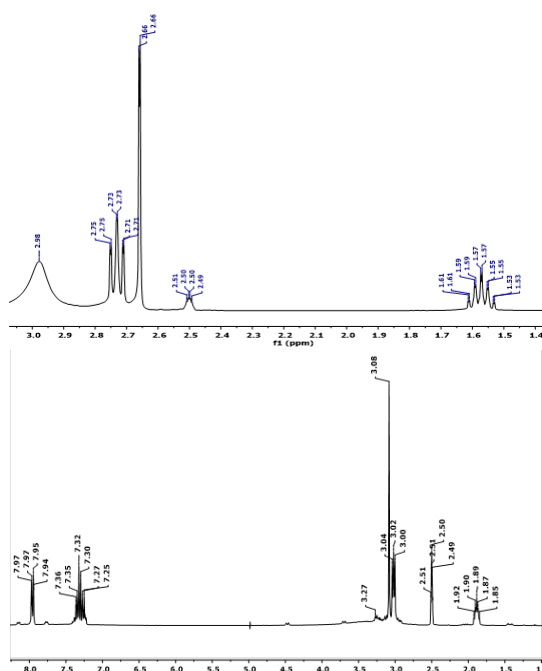
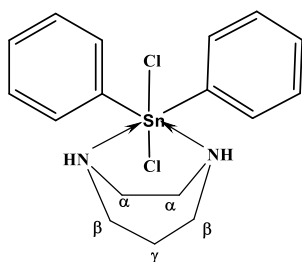


Fig. 3:  $^1\text{H}$  NMR spectrum of homopiperazine and complex.

Table 1.  $^1\text{H}$  NMR ( $\delta$ , ppm) of homopiperazine and its complex.

Protons	Free HP	Complex
2NH	2.98 (br)	3.27
2CH <sub>2</sub> ( $\alpha$ )	2.71, 2.73, 2.75	3.00, 3.02, 3.04
2CH <sub>2</sub> ( $\beta$ )	2.66	3.08
CH <sub>2</sub> ( $\gamma$ )	1.53-1.61 (m)	1.85-1.92 (m)
CH (aromatic)	-	7.25-7.36 (m), 7.94-7.97(m)



Scheme 1: Structural formula of homopiperazine complex

The thermogravimetric analysis for the complex was carried out within a temperature range from room temperature up to 600 °C, Fig. 4. The percentage mass loss and thermal effects accompanying the changes in the solid complex on heating are shown in Table 2. The TGA curve shows three steps. The first step shows the loss of a 2Cl between 99 - 179°C,

2C<sub>6</sub>H<sub>5</sub> between 179 - 270°C and HP between 270 - 430. The residue of 26.74 % is corresponding to Sn, which has a theoretical value of 26.72%.

Table 2. TGA mass loss of (C<sub>6</sub>H<sub>5</sub>)<sub>2</sub>SnCl<sub>2</sub>-HP complex in the temperature range ~25 to 600°C with a heating rate of 10 degrees/min.

Assignment Loss	TGA °C	DrTGA °C	%Wt Loss Found (Calcd)
2Cl	99-179	164	15.97 (15.92)
2C <sub>6</sub> H <sub>5</sub>	179-270	214	34.73 (34.75)
HP	270-430	359	22.52 (22.61)
Remaining Sn	> 430		26.74 (26.72)

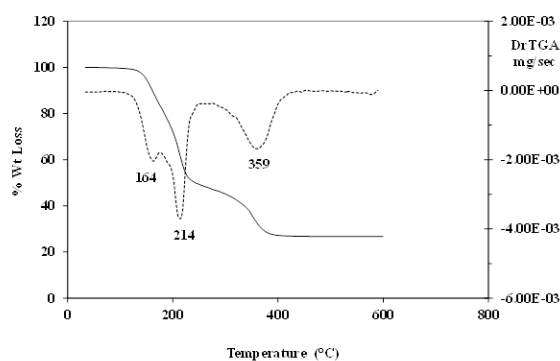


Fig. 4: Thermogravimetric analysis for diphenyltin(IV) complex with homopiperazine.

### 3.2. Complex formation equilibria

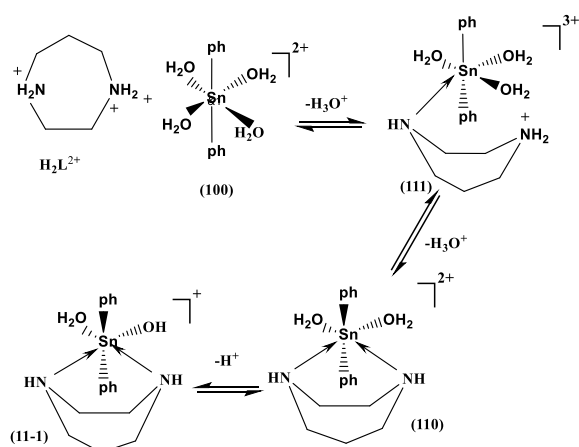
The acid-dissociation constants of the protonated homopiperazine were estimated under the same experimental conditions of ionic strength, temperature and solvent composition which are used for the study of organotin complex equilibria, Table 2. The overall protonation constants ( $\log\beta_{11}$  and  $\log\beta_{12}$ ) were calculated. The values obtained agree with the literature data [40] after considering changes in the experimental condition.

The hydrolysis of diorganotin(IV) cation in an aqueous solution was extensively studied [41-45]. The hydrolysis data of diphenyltin(IV) were fitted assuming the formation of 10-1 and 10-2 species, Table 2. The polymeric species formed in the dialkyltin(IV) hydrolysis were not detected. This may be related to the lower solubility of these species in case of diphenyltin(IV) hydrolysis. The hydrolysis constants are included in Table 2.

The potentiometric titration curves of the protonated homopiperazine in the absence and presence of diphenyltin (IV) are compared. The complex titration curve is lowered from the homopiperazine curve, Fig. 4. This may be explained

on the premise that the formation of a complex species is associated with the release of hydrogen ions. The titration data at 25°C were fitted considering the formation of the 110,111 and 11-1 species, Table 2, according to scheme 1.

The pKa of the protonated species (111) is 4.90, calculated by Eq (3). The value is less than that of free protonated homopiperazine due to coordination to tin metal ion.



Scheme 2: Complex Formation Equilibria for Diphenyltin(IV)-Homopiperazine complex

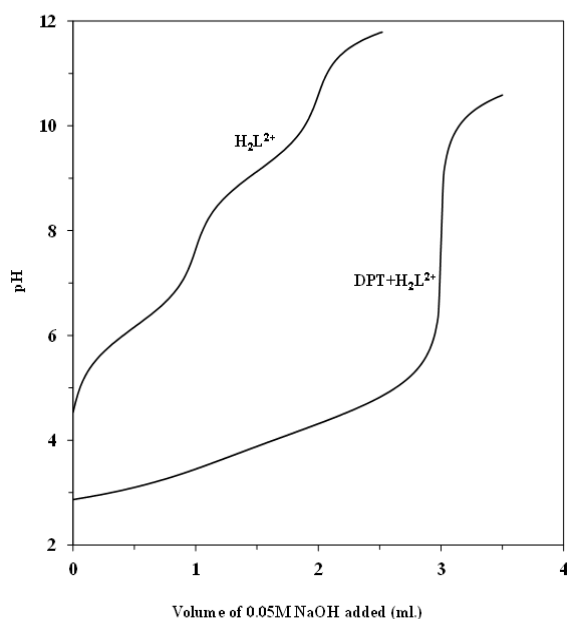


Fig. 5: Potentiometric titration curves of diphenyltin(IV)-homopiperazine system.

$$pK_a(\text{coordinated HP}) = \log\beta_{111} - \log\beta_{110} \quad (3)$$

The pKa of one of the coordinated water molecule is calculated to be 4.61 at 25°C by Eq (4) [46,47]. This value is less than that of free uncoordinated water

molecules. This may be discussed on the premise that the coordinated water molecule will be more acidic with lower pKa.

$$pK_a(\text{coordinated } H_2O) = \log\beta_{110} - \log\beta_{11-1} \quad (4)$$

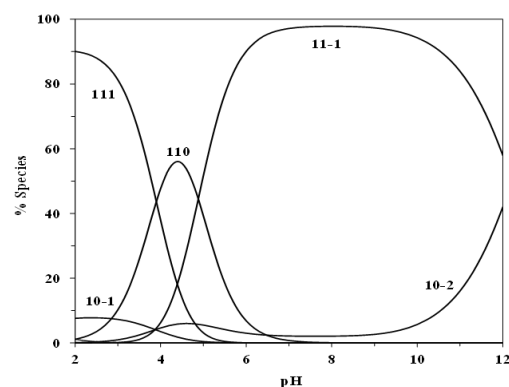


Fig. 6: Species concentration distribution as a function of pH in the diphenyltin(IV) - homopiperazine system.

Table 3. Formation constants of protonated homopiperazine and diphenyltin(IV)-HP complex in 75% Dioxane-water mixture at 25 °C.

M	L	Ha	log $\beta$ b	M	L	Ha	log $\beta$ b
0	1	1	9.13(0.01)	1	1	0	15.24(0.02)
0	1	2	15.29(0.02)	1	1	1	19.14(0.03)
1	0	-1	-1.18(0.02)	1	1	-1	10.63(0.05)
1	0	-2	-5.06(0.03)				

aM, L and H are the stoichiometric coefficients corresponding to diphenyltin(IV), HP and  $H^+$ , respectively; bStandard deviations are given in parentheses; Sums of a square of residuals are less than  $5 \times 10^{-7}$ .

The speciation diagram of diphenyltin(IV)-homopiperazine complex provides a useful picture of the homopiperazine binding with diphenyltin(IV) in media of different pH values, Fig. 6. The protonated complex, 111, predominates at lower pH up to pH = 4.0. The deprotonated complex 110 predominates in the pH range 4.0 – 5.0, with a maximum concentration of 56.1% at pH = 4.4. The hydrolyzed form 11-1 prevails after pH 5.0 with a maximum formation percentage of 97.8%. It is interesting to find that the main species in the physiological pH range is the monohydroxo species, 11-1. Therefore, the interaction of DPT complex with DNA constituent, the main target in the chemotherapy is quite feasible.

### 3.2. Molecular DFT Calculation of HP and its Complex.

The natural charges calculated from Natural Bond Orbital Analysis (NBO) of the lowest energy configurations of homopiperazine shows that the most negative centres are in N1 (-0.683) and N2 (-0.683), Figure 7. This indicates that diphenyltin(IV) prefers bidentate coordination to N1 and N2 forming 5 and 6-membered rings. Figure 8, shows the optimized structure of the complex having the lowest energy. The natural charges computed from the NBO-analysis on the coordinated atoms are Sn (+2.162), N1 (-0.748), N2 (-0.746), C11 (-0.657), C12 (-0.664), C6 (-0.591) and C12 (-0.593), Figure 7.

The Sn atom is six-coordinate in an octahedral geometry with some distortion. The atoms N1, N2, C12 and C6 are almost in one plane deviated by 1.332°, Table 4.

Figure 7 shows the change of the structure of HP ring from free ligand to its complex, where the homopiperazine ring changed from chair to boat shape. This is evidenced considering the N1- - N2 distance in free homopiperazine calculated to be 3.149 Å. This is decreased to 2.585 Å in the complex. Bonds connected to N atoms are elongated upon complex formation. This is probably due to the complexation through two NH groups of HP.

The bond lengths N1-C1, N1-C4, N1-C5, N2-C3, N2-C6 and N2-C7 are elongated by ~0.039 to 0.049 Å upon complex formation compared to those of free ligand, Table 3. The angles attached to N1 (C1-N1-C4, C1-N1-C5 and C4-N1-C5) and N2 (C3-N2-C6, C3-N2-C7 and C6-N2-C7) are decreased upon complex formation compared to those of free ligand, Table 4.

**Table 4.** Important optimized bond lengths (Å) and bond angles (°) of complex.

Type of bond	Bond length (Å)		Type of bond	Bond length (Å)	
	HP	complex		HP	complex
Sn-N1	-	2.417	N1-C1	1.464	1.513
Sn-N2	-	2.424	N1-C4	1.461	1.500
Sn-C11	-	2.600	N2-C3	1.467	1.512
Sn-C12	-	2.603	N2-C5	1.460	1.500
Sn-C6	-	2.173			
Sn-C12	-	2.172	N1- - - N2	3.149	2.585
Type of Angle	Angle (°)		Type of Angle	Angle (°)	
	HP	complex		HP	complex
N1-Sn-N2	-	64.55	C12-Sn-C6	-	92.19
N1-Sn-C6	-	88.47	C12-Sn-C12	-	91.54
N2-Sn-C12	-	88.89			
C6-Sn-C12	-	118.1	N1-Sn-C12	-	153.3
C11-Sn-N1	-	89.60	N2-Sn-C6	-	153.0
C11-Sn-N2	-	88.42	C11-Sn-C12	-	172.8
C11-Sn-C6	-	90.46			
C11-Sn-C12	-	92.00	C1-N1- C4	118.1	111.7
C12-Sn-N1	-	84.46	C3-N2- C5	116.3	111.6
C12-Sn-N2	-	85.44	N1-N2-C12-C6	-	1.332*

\*dihedral angle

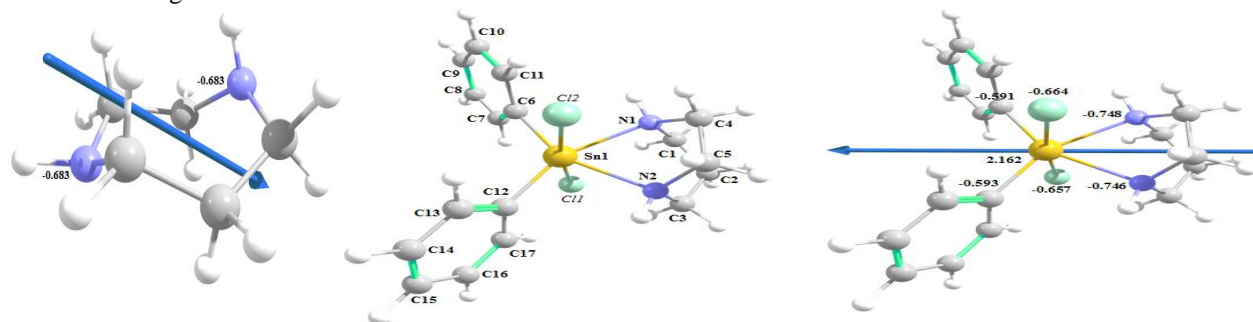


**Fig. 7.** The lowest energy structure, the charges on active centers, and the dipole moment vector of HP and complex using B3LYP.

The computed total energy, HOMO (the highest occupied molecular orbital) energies, LUMO (the lowest unoccupied molecular orbital) energies and the dipole moment for the ligand and complex were calculated in Table 5. The complex is more stable than HP. This is explained based on the results of the total energy calculation, where the total energy of the complex is more negative than that of free homopiperazine. Also, the energy gap ( $E_g$ ) =  $E_{LUMO} - E_{HOMO}$  is smaller in the case of complex than that of ligand due to chelation of ligand to metal ions, Table 5 and Fig. 8. The lowering of  $E_g$  in complex compared to that of ligand demonstrates the charge transfer interactions upon complex formation.

**Table 5.** Calculated energies of ligand and its complexes at B3LYP/LANL2DZ.

<sup>a</sup>E: the total energy (a.u.). <sup>b</sup>HOMO: highest occupied molecular orbital (eV).

<sup>c</sup>LUMO: lowest unoccupied molecular orbital (eV).

<sup>d</sup> $E_g = E_{LUMO} - E_{HOMO}$  (eV). <sup>e</sup> dipole moment (Debye).

	$E^a$	HOMO <sup>b</sup>	LUMO <sup>c</sup>	$E_g^d$	Dipole moment <sup>e</sup>
HP	-307.328	-5.8997	-0.3461	5.5536	1.6952
Complex	-1694.44	-6.7126	-1.0101	5.7025	7.1259

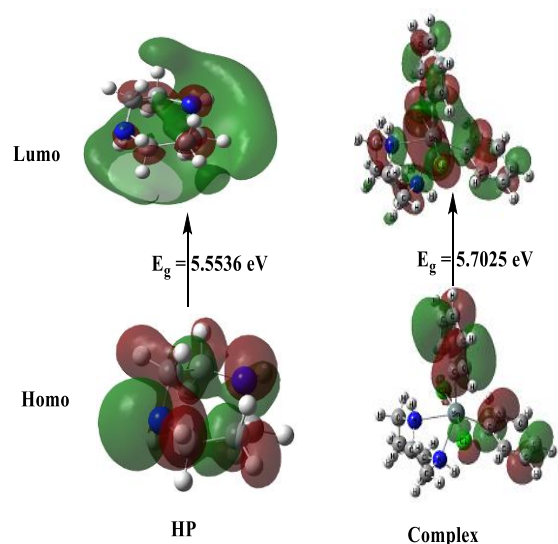


**Fig. 8.** HOMO and LUMO charge density maps of HP and complex.

### 3.2.3. Reactivity studies

Many reactivity descriptors, as electron affinity (A), ionization potential (I), Electronegativity ( $\chi$ ), electrophilicity index ( $\omega$ ), hardness ( $\eta$ ), softness (S) and chemical potential ( $\mu$ ), all derived from the

HOMO and LUMO energies, have been proposed for understanding various aspects of reactivity associated with chemical reactions, Table 6.

HP is a better electron donor than its complex because it has the highest  $E_{HOMO}$  value (lowest ionization potential). Complex is a better electron acceptor than HP, because it has lower  $E_{LUMO}$  values (higher electron affinities) than HP, Tables 5 and 6. Furthermore, Complex has higher electrophilicity ( $\omega$ ) than HP, the former molecule is electron acceptors and HP is an electron donor.

**Table 6.** The ionization energy, I, electron affinity, A, electronegativity,  $\chi$ , global softness, S, chemical hardness,  $\eta$ , and chemical potential,  $\mu$ , calculated for HP and DBT(HP)Cl<sub>2</sub>.

	HP	Complex
ionization potential $I = -E_{HOMO}$	5.8997	6.7126
electron affinity $A = -E_{LUMO}$	0.3461	1.0101
Electro-negativity $\chi = (I + A)/2$	3.1229	3.8613
chemical hardness $\eta = (I - A)/2$	2.7768	2.8512
chemical softness $S = 1/2\eta$	0.1801	0.1754
chemical potential $\mu = -\chi$	-3.1229	-3.8613
Electro-philicity $\omega = \mu^2/2\eta$	1.7561	2.6146

### 3.3. Biological activity

The screening results of antibacterial and antifungal activity of diphenyltin(IV) dichloride, homopiperazine and complex are presented in Table 6 and Figs. 9. These results revealed markedly high activity of the complex. The high activity in the complex is due to coordination which lowers the polarity [48,49] of the metal ion. The lowering is mainly due to the participation of the positive charge of Sn(IV) with the donor groups of homopiperazine in bonding. This will enhance its permeation through the lipid layer of the membrane of the microorganism and improves the biological activity.

The in vitro antitumor activity of the homopiperazine complex shows that the complex exhibits a low IC<sub>50</sub> value for breast cancer (Mcf7 cell line), Figure 10. The activity order is complex (27  $\mu$ g/ml) < homopiperazine (30  $\mu$ g/ml) < (C<sub>6</sub>H<sub>5</sub>)<sub>2</sub>SnCl<sub>2</sub> (80  $\mu$ g/ml).

**Table 7.** Antibacterial and Antifungal activity of homopiperazine and diphenyltin(IV) dichloride complex.

Sample	Inhibition zone diameter (mm / mg sample)	
	Bacteria	
	<i>Escherichia Coli</i> (G <sup>-</sup> )	<i>Staphylococcus aureus</i> (G <sup>+</sup> )
Control: DMSO	0.0	0.0
Tetracycline Antibacterial agent	34	31
HP	12	13
(C <sub>6</sub> H <sub>5</sub> ) <sub>2</sub> SnCl <sub>2</sub>	14	15
Complex	16	18
	Fungi	
	<i>Aspergillus flavus</i>	<i>Candida albicans</i>
Control: DMSO	0.0	0.0
Amphotericin B Antifungal agent	18	19
HP	11	10
(C <sub>6</sub> H <sub>5</sub> ) <sub>2</sub> SnCl <sub>2</sub>	14	11
Complex	16	12

The 2D and 3D plots of the interaction of HP, (C<sub>6</sub>H<sub>5</sub>)<sub>2</sub>SnCl<sub>2</sub> and Complex with the active site of the receptor of breast cancer oxidoreductase (PDB ID: 3HB5) are shown in Figures 11.

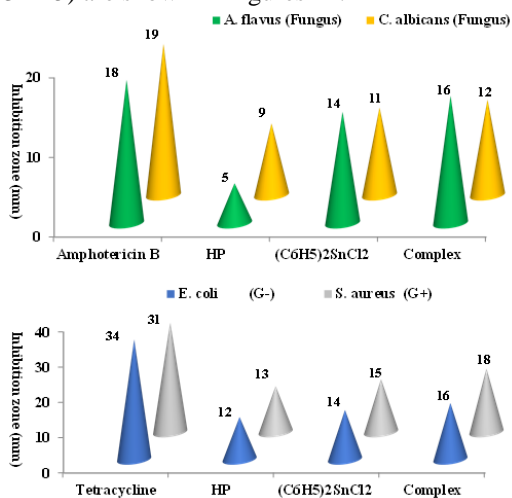


**Fig. 9.** Antibacterial and antifungal activities of homopiperazine, (C<sub>6</sub>H<sub>5</sub>)<sub>2</sub>SnCl<sub>2</sub>, and complex.

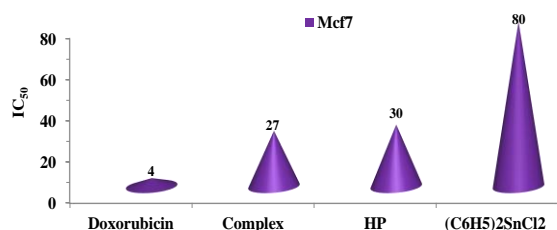


**Fig. 10.** Antitumor activity of homopiperazine, (C<sub>6</sub>H<sub>5</sub>)<sub>2</sub>SnCl<sub>2</sub>, and complex.

### 3.4. Molecular docking

#### 3.4.1. Docking on breast cancer oxidoreductase (PDB ID: 3HB5)

The binding free energy of homopiperazine, diphenyltin(IV) dichloride and the complex with protein (PDB ID: 3HB5) receptor are found to be -5.0, -1.4 and -13.8 kcal/mol for HP, (C<sub>6</sub>H<sub>5</sub>)<sub>2</sub>SnCl<sub>2</sub> and Complex; respectively, Table 7. The more negative the binding energy the more effective interaction [50]. So, the interactions are in the order of (C<sub>6</sub>H<sub>5</sub>)<sub>2</sub>SnCl<sub>2</sub> < HP < complex, Table 7.

#### 3.4.2. Docking on gram -ve bacteria: *Staphylococcus aureus* (PDB ID: 1jjj)

The results are given in Table 8 and Figure 12. The binding free energy of homopiperazine, diphenyltin(IV) dichloride and complex with protein (PDB ID: 1jjj) receptor are found to be -3.1, -4.8 and -21.2 kcal/mol for HP, (C<sub>6</sub>H<sub>5</sub>)<sub>2</sub>SnCl<sub>2</sub> and complex; respectively, Table 8. The more negative the binding energy the stronger interaction. So, the interactions are in the order of HP < (C<sub>6</sub>H<sub>5</sub>)<sub>2</sub>SnCl<sub>2</sub> < complex.

The 2D and 3D plots of the interaction of HP, (C<sub>6</sub>H<sub>5</sub>)<sub>2</sub>SnCl<sub>2</sub> and complex with the active site of the receptor of *Staphylococcus aureus* (gram +ve bacteria) (PDB ID: 1jjj) are shown in Figures 12.

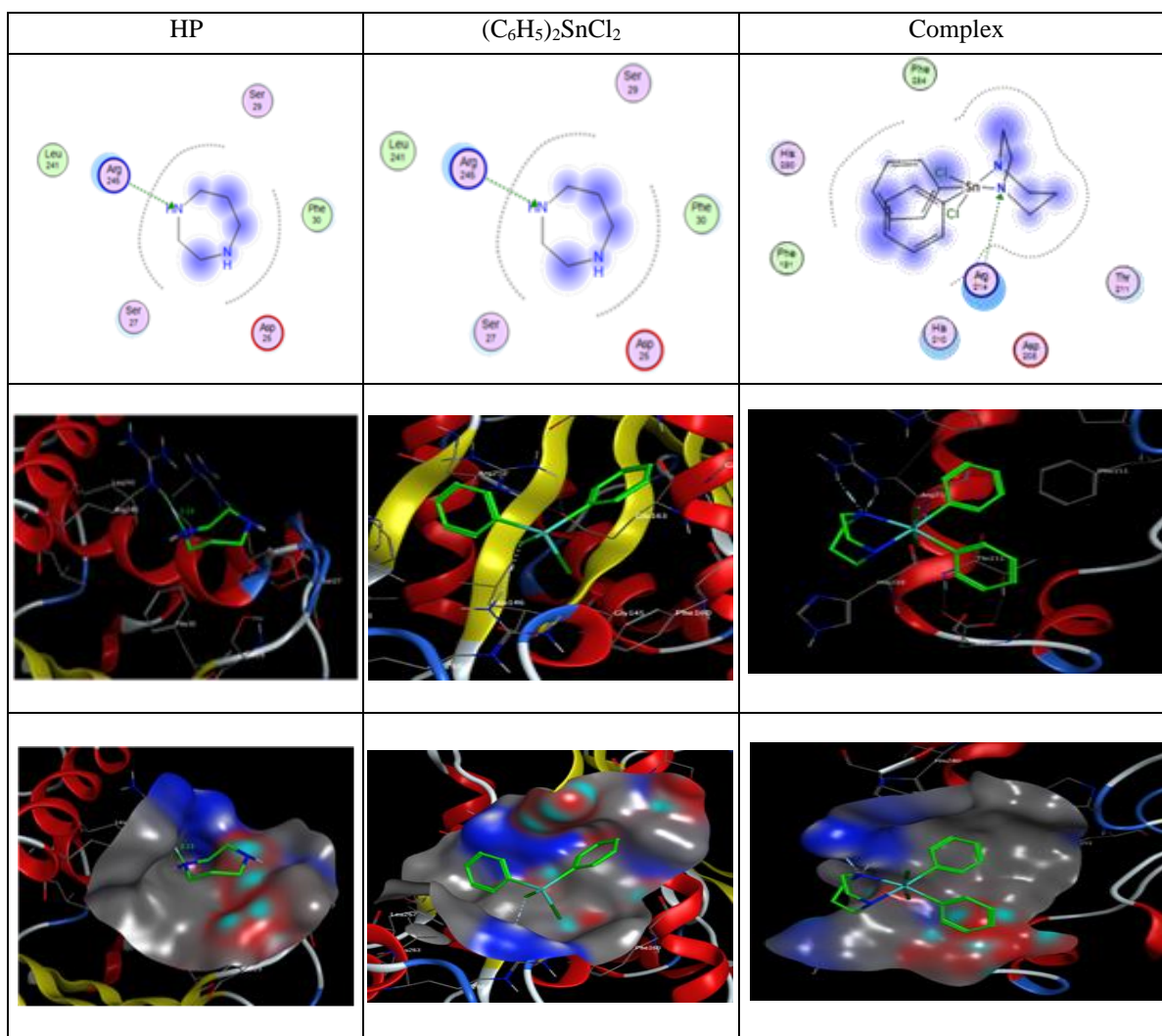
## 4. Conclusions

The homopiperazine complex with diphenyltin(IV) was investigated. The solid complex was synthesized with stoichiometric ratio of 1:1. The structure of the solid complex was evidenced by elemental analysis, thermal techniques and spectral measurements as mass, IR and NMR. The complex formation equilibria were studied. The detected species in solution are the 1:1 complex together with protonated and hydrolysed forms. The formation constants were determined and the speciation diagrams were evaluated. The optimization of the complex structure was estimated by DFT calculations. The Sn atom is six coordinate in a distorted octahedral geometry, where the two nitrogen atoms of homopiperazine and the two chloride ions are in one plane. The biological activities as antibacterial, antifungal and antitumor were tested. Docking studies estimated the possible modes of binding of diphenyltin(IV), homopiperazine and complex to the most active sites of the breast cancer oxidoreductase receptor and those of *Escherichia coli*.

**Table 7.** The Docking interaction data calculations of HP,  $(C_6H_5)_2SnCl_2$  and Complex with the active site of the receptor of breast cancer oxidoreductase (PDB ID: 3HB5).

	Receptor		Interaction	Distance( $\text{\AA}$ )*	E (Kcal/mol)
HP					
N 2	NE	ARG 245	H-acceptor	3.06	-5.0
$(C_6H_5)_2SnCl_2$					
Cl 3	NH1	ARG 266	H-acceptor	3.47 (2.52)	-1.0
Cl 2	O	GLY 145	ionic	3.33	-0.4
Complex					
N 2	NE	ARG 214	H-acceptor	3.32 (2.41)	-4.4
N 2	NH2	ARG 214	H-acceptor	3.18 (2.24)	-9.4

\*The lengths of H-bonds are in brackets.

**Fig. 11.** 2D and 3D plots of the interaction between HP,  $(C_6H_5)_2SnCl_2$  and Complex with the active site of the receptor of breast cancer oxidoreductase (PDB ID: 3HB5). Hydrophobic interactions with amino acid residues are shown with dotted curves.

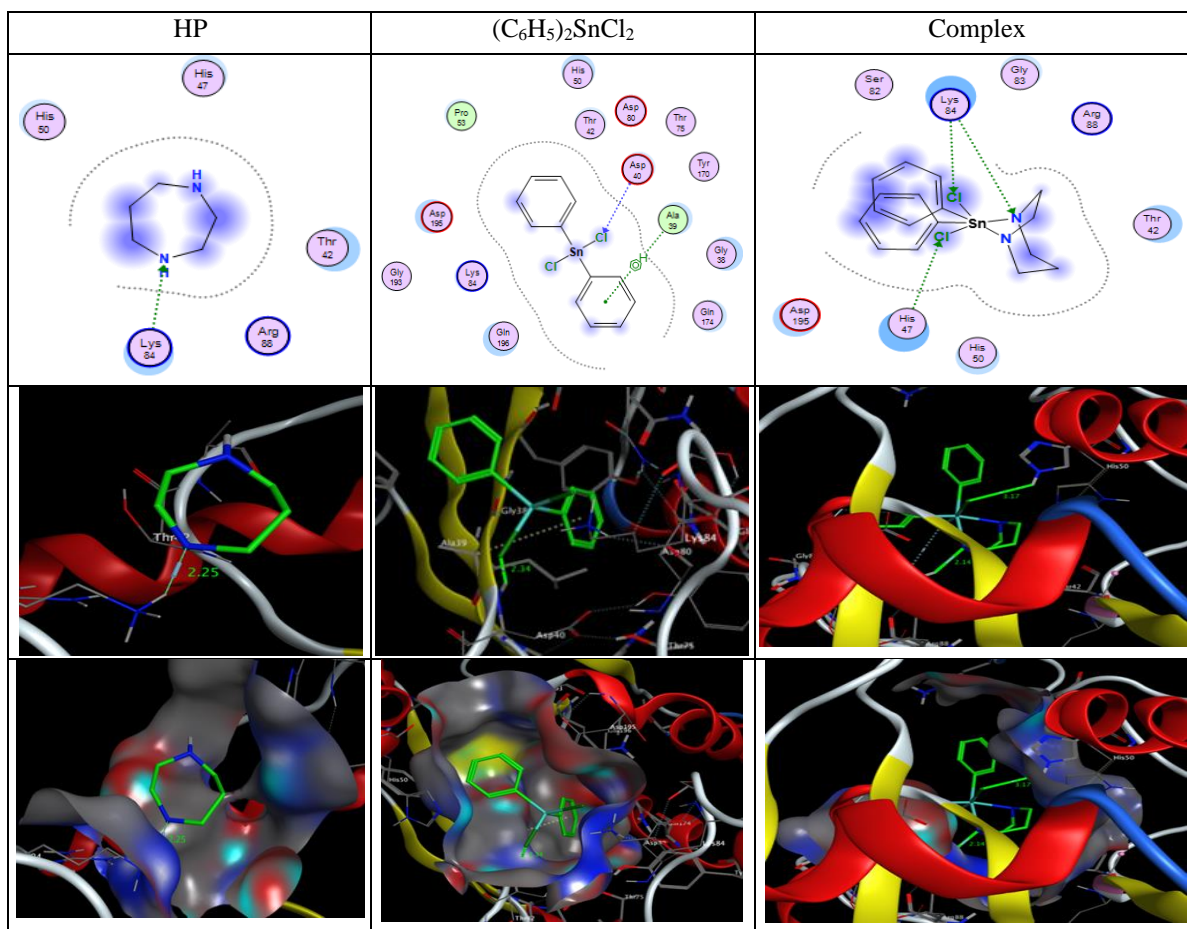


**Fig. 12.** 2D and 3D plots of the interaction between HP,  $(C_6H_5)_2SnCl_2$  and Complex with the active site of the receptor of *Staphylococcus aureus* (gram +ve bacteria) (PDB ID: 1jjj). Hydrophobic interactions with amino acid residues are shown with dotted curves.

**Table 8.** The Docking interaction data calculations of HP,  $(C_6H_5)_2SnCl_2$  and with the active sites of the receptor of *Staphylococcus aureus* (gram +ve bacteria) (PDB ID: 1jjj).

	Receptor		Interaction	Distance(Å)*	E (Kcal/mol)
HP					
N 1	NZ	LYS 84	H-acceptor	3.20 (2.25)	-3.1
$(C_6H_5)_2SnCl_2$					
Cl 3	OE1	GLU 278	H-donor	3.17	-3.2
6-ring	CA	GLY 275	pi-H	4.09	-0.8
6-ring	N	LYS 276	pi-H	3.82	-0.8
Complex					
N 1	NZ	LYS 84	H-acceptor	3.07 (2.14)	-19.8
Cl 19	NE2	HIS 47	H-acceptor	3.88 (3.17)	-0.8
Cl 20	CE	LYS 84	H-acceptor	4.01 (3.10)	-0.6

\*The lengths of H-bonds are in brackets

## 5. Conflicts of interest

There are no conflicts to declare.

## 6. References

- [1] Gielen M., Dalil H., Biesemans M., Mahieu B., de Vos D., Willem R., Di and Tri-organotin Derivatives of 3S,4S-3-[(R)-1-

- (tertbutyldimethylsilyloxy)ethyl]-4-[(R)-1-carboxyethyl]-2-azetidinone: Synthesis, Characterization and In Vitro Antitumour Activity. *Appl Organomet Chem.*, 13: 515–520 (1999). DOI:10.1002/(sici)1099-0739(199907)13:7<515::aid-aoc875>3.0.co;2-b
- [2] Gielen M, Tiekink E.R.T., Tin Compounds and Their Therapeutic Potential, in *Metallotherapeutic Drugs and Metal-Based Diagnostic Agents, the Use of Metals in Medicine*. West Sussex, United Kingdom: J. Wiley & Sons, 421–439(2005). DOI:10.1002/0470864052
- [3] Alama A., Tasso B., Novelli F., Sparatore F., Organometallic Compounds in Oncology: implications of Novel Organotins as Antitumor Agents. *Drug Discov.*, 14: 500–508(2009). DOI:10.1016/j.drudis.2009.02.002
- [4] Hadjikakou S.K., Hadjiliadis N., Antiproliferative and Anti-tumor Activity of Organotin Compounds. *Coord Chem Rev.*, 253: 235–249 (2009). DOI:10.1016/j.ccr.2007.12.026
- [5] Awang N., Kamaludin N.F., Ghazali A.R., Cytotoxic Effect of Organotin(IV) Benzylosopropylthiocarbamate on Chang Liver Cell and Hepatocarcinoma hepG2 Cell. *Pak J Biol Sci.*, 14(15): 768–774(2011). DOI:10.3923/pjbs.2011.768.774
- [6] Niu L., Li Y., Li Q., Medicinal Properties of Organotin Compounds and Their Limitations Caused by Toxicity. *Inorg Chim Acta*, 423: 2–31(2014). DOI:10.1016/j.ica.2014.05.007.
- [7] Sedaghat T., Golalzadeh A., Motamedi H., Diorganotin Complexes with N(4)-Phenylthiosemicarbazones: Synthesis, Spectroscopic Characterization, and Antibacterial Activity. *Phosphorus Sulfur Silicon Relat Elem.*, 188: 1694–1702(2013). DOI:10.1080/10426507.2013.777727.
- [8] Najeeb D., Shalan N., Ibraheem H., Farina Y., Yousif E., Synthesis and Fungicidal Activity of Some Diorganotin(IV) with Benzamidocysteine. *Alnahrain Univ.*, 12(1): 24–28(2009). DOI:10.22401/JNUS.12.1.04
- [9] Jain M., Gaur S., Singh V.P., Singh R.V., Organosilicon (IV) and Organotin (IV) Complexes as Biocides and Nematicides: Synthetic, Spectroscopic and Biological Studies of N\N Donor Sulfonamide Imine and its Chelates. *Main Gr Met Compd.*, 18: 73–82(2004). DOI:10.1002/aoc.573
- [10] Attanzio A., Agostino S. D., Busà R., Frazzitta A., Rubino S., Girasolo M.A., et al., Cytotoxic Activity of Organotin(IV) Derivatives with Triazolopyrimidine Containing Exocyclic Oxygen Atoms. *Molecules*, 25 (859) :1–16(2020). DOI:10.3390/molecules25040859.
- [11] Jan C.R., Jiann B.P., Lu Y.C., Chang H.T., Su W., Chen W.C., et al., Effect of the Organotin Compound Triethyltin on Ca<sup>2+</sup> Handling in Human Prostate Cancer Cells. *Life Sci.*, 70 (11) : 1337–1345(2002). DOI:10.1016/s0024-3205(01)01500-4
- [12] Samuel M.P., de Vos D., Raveendra D., Sarma J.A.R.P., Roy S., 3-D QSAR Studies on New Dibenzyltin(IV) Anticancer Agents by Comparative Molecular Field Analysis (CoMFA). *Bioorg Med Chem Lett.*, 12(1): 61–64(2002). DOI:10.1016/S0960-894X(01)00684-9
- [13] Shuaibu M.N., Kanbara H., Yanagi T., Ichinose A., Ameh D.A., Bonire J.J., Nok A.J., In Vitro trypanocidal Activity of Dibutyltin Dichloride and its Fatty Acid Derivatives. *Parasitol. Res.*, 91(1): 5–11(2003). DOI:10.1007/s00436-003-0861-2
- [14] Tabassum S., Pettinari C., Chemical and Biotechnological Developments in Organotin Cancer Chemotherapy. *J Organomet Chem.*, 691:1761–1766(2006). DOI:10.1016/j.jorganchem.2005.12.033.
- [15] Florea A.M., Busselberg D., Cisplatin as an Anti-tumor Drug: Cellular Mechanisms of Activity, Drug Resistance and Induced Side Effects. *Cancers*, 3: 1351–1371(2011). DOI:10.3390/cancers3011351
- [16] Deo K.M., Ang D.L., McGhie B., Rajamanickam A., Dhiman A., Khoury A., et al., Platinum Coordination Compounds with Potent Anticancer Activity. *Coord. Chem. Rev.*, 375:148–163(2018). DOI:10.1016/j.ccr.2017.11.014
- [17] Rubino S., Pibiri I., Minacori C., Alduina R., Di Stefano V., Orecchio S., et al., Synthesis, Structural Characterization, Anti-proliferative and Antimicrobial Activity of Binuclear and Mononuclear Pt(II) Complexes with Perfluoroalkyl-Heterocyclic Ligands. *Inorg Chim Acta*, 483: 180–190(2018). DOI:10.1016/j.ica.2018.07.039.

- [18] Sirajuddin M., Ali S., Tahir M.N.. Pharmacological Investigation of Mono-, Di- and tri-Organotin(IV) Derivatives of Carbodithioates: Design, Spectroscopic Characterization, Interaction with SS-DNA and POM Analyses. *Inorg Chim Acta*, 439: 145–158(2016). DOI:10.1016/j.ica.2015.10.017.
- [19] Hadi A.G., Jawad K., Ahmed D.S., Yousif E., Synthesis and Biological Activities of Organotin (IV) Carboxylates: A Review. *Sys Rev Pharm.*, 10 (1): 26–31(2019). DOI:10.5530/srp.2019.1.5
- [20] Al Alousi A.S., Shehata M.R., Shoukry M.M., Mohamed N.M., Chem., Interaction of dimethyltin(IV) and trimethyltin(IV) with dehydroacetic acid. *Speciat. Bioavailab.*, 21 : 1–6(2009). DOI: 10.3184/095422909X41621
- [21] Shehata M.R., Mohamed M.M.A., Shoukry M.M., Hussein M.A., Hussein F.M., Synthesis, characterization, equilibria and biological activity of dimethyltin (IV) complex with 1,4-piperazine. *J Coord Chem.*, 68:1101-1114(2015). DOI: 10.1080/00958972.2015.1007962
- [22] Alnajjar A.A., Mohamed M.M.A., Shoukry M.M., Interaction of dipropyltin(IV) with amino acids, peptides, dicarboxylic acids and DNA constituents. *J. Coord. Chem.*, 59: 193-206(2006). DOI: 10.1080/00958970500270786
- [23] Hassan S. S., Shoukry M. M., Jbarah A. Q., Coordination Compound of Dimethyltin(IV) with N,N,N',N' Tetraethylethylenediamine: Speciation and Theoretical approach , *J. Mex. Chem. Soc.*, 64(2): (2020) Regular Issue ©2020, Sociedad Química de México ISSN-e 2594-0317. DOI: [10.29356/jmcs.v64i2.1079](https://doi.org/10.29356/jmcs.v64i2.1079)
- [24] Al-Flajj O., Shehata M.R., Mohamed M.M.A., Shoukry M.M., Interaction of dimethyltin (IV) with DNA constituents. *Monatshefte fur Chemie*, 132: 349–366(2001). DOI: 10.1007/s007060170121
- [25] El-Sherif A.A., Shehata M.R., Shoukry M.M., Mahmoud N., Potentiometric Study of Speciation and Thermodynamics of Complex Formation Equilibria of Diorganotin (IV) Dichloride with 1-(2-Aminoethyl) piperazine. *J Sol Chem.*, 45: 410-430(2016). DOI: 10.1007/s10953-016-0450-5
- [26] Shoukry M.M., Khairy E.M., Mohamed M.M.H., Equilibrium studies of organotin(IV) complexes with vitamin B6. *Talanta*, 44: 1149-1157(1997). DOI: 10.1016/S0039-9140(96)02113-3
- [27] Mohamed M.M.A., Shehata M.R., Shoukry M.M., Trimethyltin (IV) complexes with some selected DNA constituents. *J Coord Chem.*, 53:125-142(2001). DOI: 10.1080/00958970108022607
- [28] Shoukry M.M., Potentiometric studies of the complex formation between trimethyltin (IV) and some selected amino acids. *J Inorg Biochem.*, 48: 271-277(1992). DOI:10.1016/0162-0134(92)84053-P
- [29] Shoukry M.M., Equilibrium studies of the diorganotin(IV) complexes with some amino acids and related compounds. *Talanta*, 43: 177-183(1996). DOI: 10.1016/0039-9140(95)01708-9
- [30] Bates R.G., Determination of pH: Theory and Practice. 2nd Edn. Wiley Interscience, New York (1977).
- [31] Motekaitis R.J., Martell A.E., Nelson D.A., Formation and stabilities of cobalt (II) chelates of N-benzyl triamine Schiff bases and their dioxygen complexes. *Inorg Chem.*, 23 : 275-283(1984). DOI: 10.1021/ic00171a005
- [32] Shoukry M.M., Shehata M.R., Hamza M.S.A., van Eldik R., Equilibrium, kinetic and solvent effect studies on the reactions of [Ru<sub>m</sub>(Hedta)(H<sub>2</sub>O)] with thiols. *Dalton Trans.*, 24: 3921-3926(2005). DOI: 10.1039/B510553F
- [33] Gans P., Sabatini A., Vacca A., An improved computer program for the computation of formation constants from potentiometric data. *Inorg Chim Acta*, 18 : 237-239(1976). DOI: 10.1016/s0020-1693(00)95610-x
- [34] Pettit L., Personal Communication, University of Leeds (1993).
- [35] Frisch M.J., Trucks G.W., Schlegel H.B., Scuseria G.E., Robb M.A., Cheeseman J.R., et al., Gaussian 09, Revision D.01 (Gaussian, Inc., Wallingford CT), 2013.
- [36] Inc C.C.G., "Molecular operating environment (MOE 2019.01)" Chemical Computing Group Inc. 1010 Sherbooke St. West, Suite # 910, Montreal, QC, Canada, H3A 2R7, (2019).

- [37] Jin Z., Du X., Xu Y., Deng Y., Liu M., Zhao Y., Zhang B., Li X., Zhang L., Peng C., Duan Y., Yu J., Wang L., Yang K., Liu F., Jiang R., Yang X., You T., Liu X., Yang X., Bai F., Liu H., Liu X., Guddat L.W., Xu W., Xiao G., Qin C., Shi Z., Jiang H., Rao Z., Yang H. et al., Structure of Mpro from COVID-19 Virus and Discovery of its Inhibitors. *Nature*, 582 :289–293(2020). DOI: 10.1038/s41586-020-2223-y
- [38] Qiu X., Janson C.A., Smith W.W., Green S.M., McDevitt P., Johanson K., Carter P., Hibbs M., Lewis C., Chalker A., Fosberry A., Lalonde J., Berge J., Brown P., Houge-Frydrych S.V., Jarvest R.L., Crystal structure of *Staphylococcus aureus* tyrosyl-tRNA synthetase in complex with a class of potent and specific inhibitors. *Protein Science*, 10(10): 2008-2016(2001). DOI: 10.1110/ps.18001
- [39] Bellamy L.J.F.C., The infra-red spectra of complex molecules. Springer Science & Business Media. (2013).
- [40] Pagano J.M., Goldberg D.E., Fernelius W.C., A thermodynamic study of homopiperazine, piperazine and N-(2-aminoethyl)-piperazine and their complexes with copper (II) ion. *J Phys Chem.*,65:1062-1064(1961). DOI: 10.1021/J100824A513
- [41] Arena G., Cali R., Contino A., Musumeci A., Musumeci S., Purrello R., Coordination properties of dialkyltin (IV) in aqueous solution. Thermodynamic study of dimethyltin (IV) complexes with l-amino acids. *Inorg Chim Acta*, 237:187-191(1995). DOI: 10.1016/0020-1693(95)04655-S
- [42] Natsume T., Aizawa S., Hatano K., Funahashi S., Hydrolysis, polymerisation, and structure of dimethyltin (IV) in aqueous solution. Molecular structure of the polymer  $[(\text{SnMe}_2)_2(\text{OH})_3]\text{ClO}_4$ . *J Chem Soc Dalton Trans.*,2749-2753(1994). DOI: 10.1039/DT9940002749
- [43] Buzas N., Gajda T., Nagy L., Kuzmann E., Vertes A., Burger K.. Unusual coordination behavior of D-fructose towards dimethyltin (IV): metal-promoted deprotonation of alcoholic OH groups in aqueous solutions of low pH. *Inorg Chim Acta* ,274 :167-176(1998). DOI: 10.1016/S0020-1693(97)06044-1
- [44] De Stefano C., Foti C., Gianguzza A., Martino M., Pellerito L., Sammatanov S., Hydrolysis of  $(\text{CH}_3)_2\text{Sn}^{2+}$  in different ionic media: salt effects and complex formation. *J Chem Eng Data*, 41 :511-515(1996). DOI: 10.1021/je9502915
- [45] Foti C., Gianguzza A., Millero F.J., Sammartano S., The speciation of  $(\text{CH}_3)_2\text{Sn}^{2+}$  in electrolyte solution containing the major components of natural waters. *Aquat Geochem.*, 5: 381-398(1999). DOI:10.1023/A:1009613712280.
- [46] El-Sherif A.A., Shehata M.R., Shoukry M.M., Mahmoud N.M.. Equilibrium studies of diethyltin(IV) dichloride and divinyltin(IV) dichloride with 1-(2-aminoethyl) pyrrolidine. *J. Mol. Liq.*, 262:422-434(2018). Doi: 10.1016/j.molliq.2018.02.008
- [47] Shehata M.R., Shoukry M.M., Abdel Wahab A.M.. Equilibrium studies of binary and mixed-ligand dimethyltin(IV) complexes involving homopiperazine and DNA constituents with reference to the antitumor activity. *Physics and Chem. of Liquids*, 59 :523-536(2021). Doi:10.1080/00319104.2020.175268936
- [48] Chohan Z.H., Supuran C.T., Scozzafava A., Metal binding and antibacterial activity of ciprofloxacin complexes. *J Enzyme Inhib Med Chem.*, 20: 303–307(2005). DOI: 10.1080/14756360310001624948
- [49] Chohan Z.H., Arif M., Shafiq Z., Yaqub M., Supuran C.T., In vitro antibacterial, antifungal & cytotoxic activity of some isonicotinoylhydrazide Schiff's bases and their cobalt (II), copper (II), nickel (II) and zinc (II) complexes. *J Enzyme Inhib Med Chem.*, 21 :95–103(2006).DOI: 10.1080/14756360500456806
- [50] Abdel-Rahman L.H., Basha M.T., Al-Farhan B.S., Shehata M. R., Abdalla E.M., Synthesis, characterization, potential antimicrobial, antioxidant, anticancer, DNA binding, and molecular docking activities and DFT on novel Co (II), Ni (II), VO (II), Cr (III), and La (III) Schiff base complexes. *Applied Organometallic Chemistry*, e6484 (2021). DOI: 10.1002/aoc.6484